Pneumatically Actuated Soft Wearable Exoskeleton for Upper Limb Motion Rehabilitation

A Technical Report submitted to the Department of Mechanical Engineering

Presented to the Faculty of the School of Engineering and Applied Science
University of Virginia • Charlottesville, Virginia

In Partial Fulfillment of the Requirements for the Degree
Bachelor of Science, School of Engineering

Jackson Spain
Spring, 2025
Technical Project Team Members:
Kaitlin Cole
Jahnavi Dave
Joshua Lim
Jake Morrisey
Jackson Spain
Courtney Wilks

On my honor as a University Student, I have neither given nor received unauthorized aid on this assignment as defined by the Honor Guidelines for Thesis-Related Assignments

Dr. Sarah Sun, Department of Mechanical and Aerospace Engineering

Problem Statement

Each year, around 16.9 million individuals experience a stroke, leading to approximately 33 million stroke survivors and 5.9 million deaths annually. As one of the leading causes of death globally, strokes are a significant contributor to acquired disabilities in adults. Of those, roughly 80% of stroke survivors face upper limb motor impairments. There are many therapies in practice to treat. The most effective of those is a method known as constraint-induced motor therapy (CIMT). CIMT involves restraining unaffected limbs and having the patients practice moving the affected region. Studies have shown that adding CIMT to traditional recovery methods improves patient outcomes (Zhang et al, 2023). However, only a limited number of those with upper limb disabilities are able to participate as it requires a baseline level of physical ability. This project proposes a new design for a pneumatically actuated soft wearable upper limb rehabilitative exoskeleton. The exoskeleton allows patients to achieve a level of use previously unavailable to them through current therapeutic practices. By being soft and lightweight, the exoskeleton is easily portable, meaning patients can access it from the comfort of their own home, drastically improving the quality of life and ease of recovery.

Research

Wearable devices designed to assist with upper limb motion are groundbreaking innovations that have revolutionized modern healthcare. Research has been conducted on both rigid and soft exoskeletons, but the field of soft exoskeletons is rapidly growing due to their increased durability, comfort, and flexibility (Chiaradia et al., 2020; Bardi et al., 2022; Li et al., 2017; Cappello et al., 2016). Soft exoskeletons are made of light, flexible materials like fabric or elastomers, while rigid exoskeletons have a frame made of hard materials like metal or plastic.

These devices are heavier and bulkier, but gain a higher torque rating, bandwidth, and power efficiency (Chiaradia et al., 2020). Rigid exoskeletons generate more force with greater speed compared to a soft exoskeleton. However, soft exoskeletons are lighter and more comfortable than their rigid counterparts, making them more feasible for day-to-day assistance. For this reason, engineers continue to seek innovative solutions for soft exoskeletons that can match the force and speed of current rigid exoskeletons.

There are seven degrees of freedom (DOF) in the human arm: three in the shoulder, two in the elbow, and two in the wrist. A degree of freedom is a type of movement that a joint or mechanism can make in a particular direction or plane. The three DOF in the shoulder are flexion/extension, abduction/adduction, and internal/external rotation. The two in the elbow are flexion/extension and pronation/supination, while the two in the wrist are flexion/extension and radial/ulnar deviation. Each of these DOF has a varying range of motion (ROM) listed in Table I. There are few soft robotic wearable devices that are advanced enough to reach the market, and fewer still that can successfully activate multiple degrees of freedom in the arm or sufficient range of motion to be deemed effective. Based on the findings from a thorough literature review conducted through PubMed, Scopus, and Web of Science, most devices actuate only one or two degrees of freedom (Bardi et al., 2022).

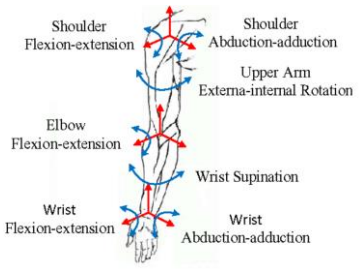

Fig. 1. DOF in Human Arm

Table I: Range of Motion for Arm DOF

	Movement	Range of Motion
Shoulder	Flexion/Extension	180°/45°
	Abduction/Adduction	150°/30°
	Internal/External Rotation	90°/90°
Elbow	Flexion/Extension	145°/0°
	Pronation/Supination	90°/90°
Wrist	Flexion/Extension	75°/75°
	Radial/Ulnar Deviation	20°/30°

Exoskeletons have been developed for three distinct scenarios: assistance, rehabilitation, and augmentation. In the assistance scenario, wearable exoskeletons are designed to support everyday activities, including eating, drinking, reaching, and hygiene. In the rehabilitative scenario, they provide repetitive movements that are typical in physical therapy exercises. In the augmentation scenario, exoskeletons enhance natural motion by providing high torques that increase human capabilities or evenly distribute the loads across the limb. The majority of devices are used for medical reasons, particularly through rehabilitation and/or assistance (Bardi et al., 2022).

Numerous actuation techniques for soft wearable exoskeletons have been studied: pneumatic, cable-driven, passive, shape memory alloy, spring blades, and hybrid. Pneumatic

actuators are favored for motion in the shoulder joint, whereas spring blades and shape memory alloy are better suited for motion in the wrist. Although cable-driven actuators are ideal for incorporating intention detection strategies and portability, pneumatic actuators offer the advantage of intrinsic compliance, meaning they can adapt to external forces and resist snapping or breaking. Both pneumatic and cable-driven actuators are commonly used for elbow joint motion, with pneumatic actuators being the most prevalent choice for shoulder joint motion (Bardi et al., 2022; Cappello et al., 2016). There is significantly less research done on intention detection strategies, though those that do tend to include the use of IMU, EMG, and EEG sensors. Those that do not include intention detection strategies either predefine the trajectory of the suit or manually make adjustments (Bardi et al., 2022). A previous capstone group utilized pneumatic actuation with the assistance of Dr. Sarah Sun, and they were able to achieve one degree of freedom (DOF) through shoulder abduction and adduction (Applegate et al., 2022). An image of their final design can be seen in Fig. 2.

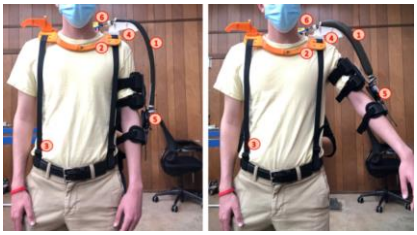

Fig. 2. 2022 Capstone

Ideation

Ideas Pre-Screening

DF

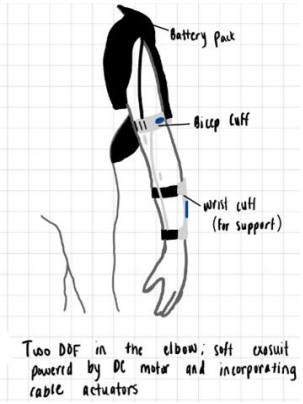

-

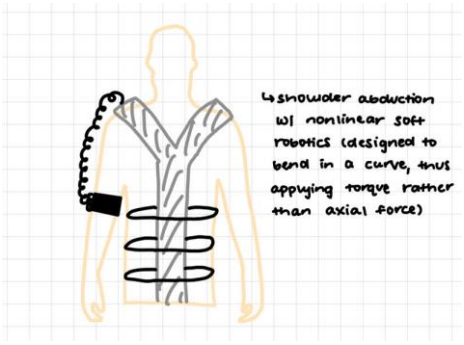

3

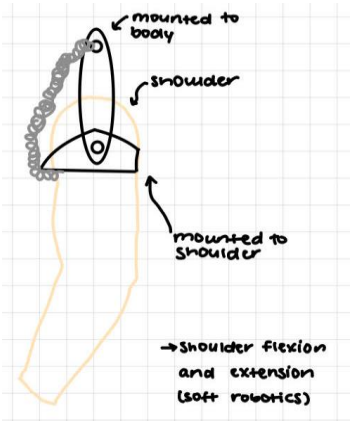

4

5

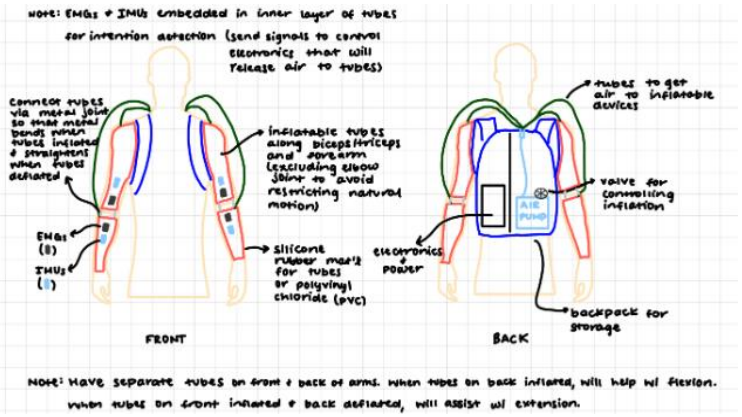
NOTE: EMGs + IMUs embedded in inner layer of tubes for intention detection (send signals to control electronics that will release air to tubes)
connect tubes via metal joint so that metal bends when tubes inflated & straightens when tubes deflated
inflatable tubes along bicep/tricep and forearm (excluding elbow joint to avoid restricting natural motion)
tubes to get air to inflatable devices
valve for controlling inflation
EMGs (■)
IMUs (■)
silicone rubber mat'l for tubes or polyvinyl chloride (PVC)
electronics & power
AIR PUMP
backpack for storage
FRONT
BACK
NOTE: Have separate tubes on front & back of arms. When tubes on back inflated, will help w/ flexion. When tube on front inflated & back deflated, will assist w/ extension.

6

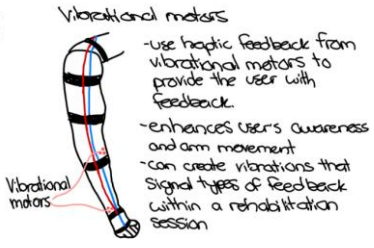
Vibrational motors
-use haptic feedback from vibrational motors to provide the user with feedback.
-enhances user's awareness and arm movement
-can create vibrations that signal types of feedback within a rehabilitation session
Vibrational motors

7

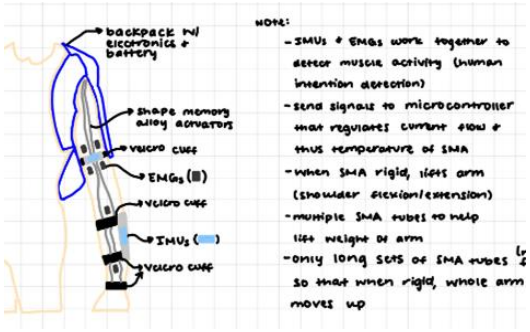
backpack w/ electronics & battery
shape memory alloy actuators
velcro cuff
EMGs (■)
velcro cuff
IMUs (■)
velcro cuff
NOTE:
- IMUs + EMGs work together to detect muscle activity (human intention detection)
- send signals to microcontroller that regulates current flow & thus temperature of SMA
- when SMA rigid, lifts arm (shoulder flexion/extension)
- multiple SMA tubes to help lift weight of arm
- only long sets of SMA tubes (
so that when rigid, whole arm moves up

8

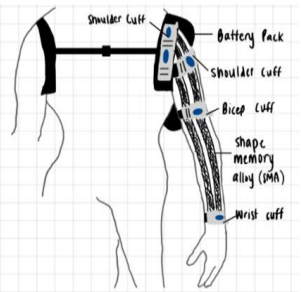

Four DOF soft exosuit with two DOFs in the shoulder, and one in the elbow and wrist each; includes shape memory alloy (SMA) that adapts to wearers skin and movements; large battery with cross-chest strap

9

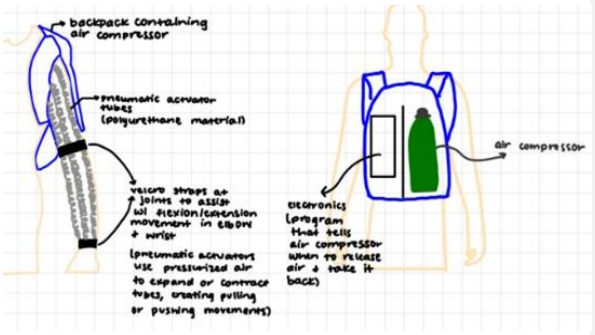

10

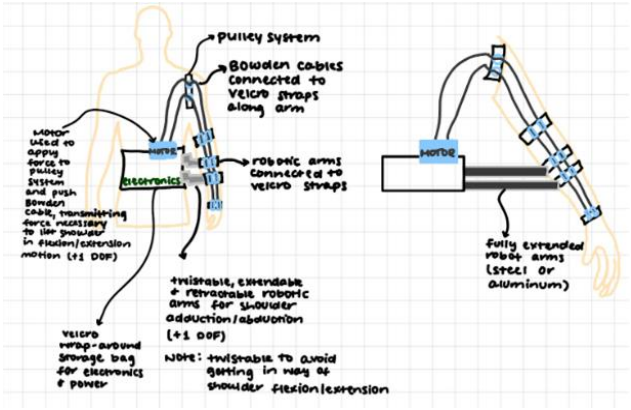

Ideas Pre-Scoring

5

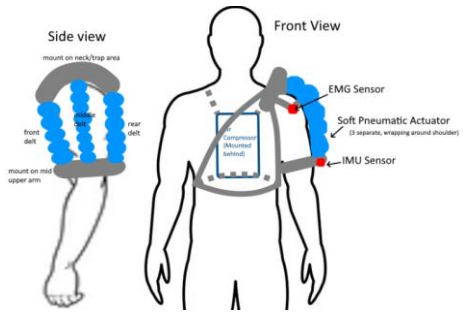

6

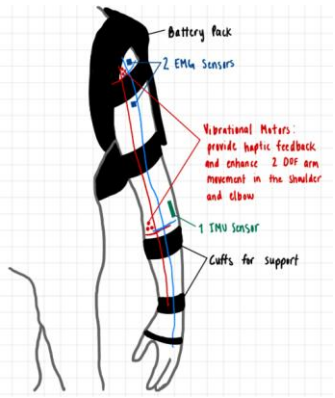

9+

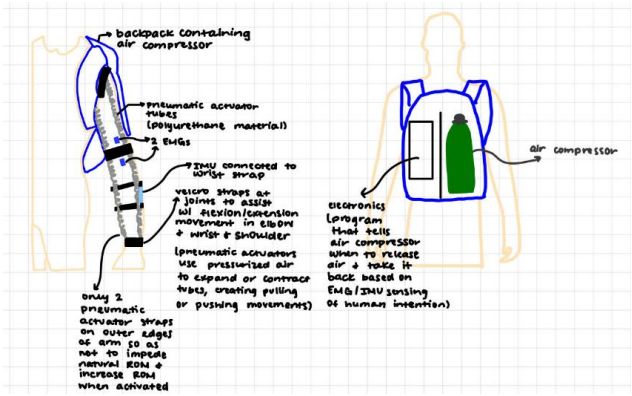

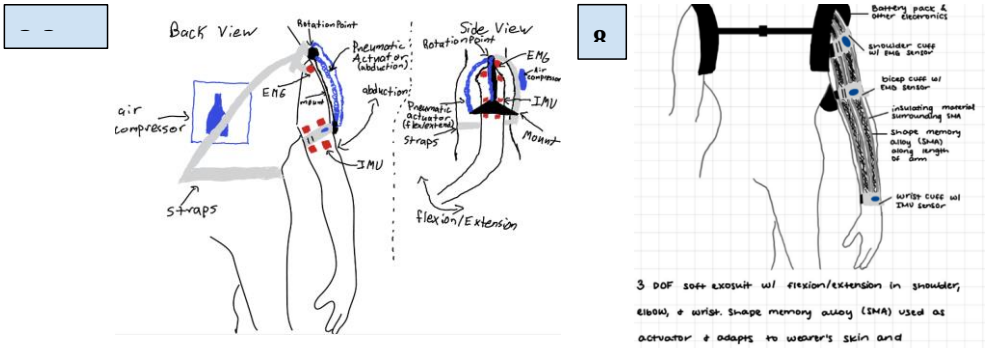

Selection and Screening

We carefully selected criteria that reflected the essential functional, practical, and user-focused features of the device to ensure it performs effectively, remains safe, and is user-friendly. The weighting emphasizes the most critical aspects, such as safety, range of motion, and degrees of freedom, while also considering factors like material composition, portability, and ease of manufacturing to balance functionality with practicality and user needs. Our reference concept (REF) was based on the 2022 capstone project's design and scored as 0 for all selection criteria, serving as a baseline for comparison, while concept variants were rated with a "-", "0," or "+" based on their performance. Key criteria such as the number of degrees of freedom (#1), lightweight design (#2), range of motion (#6), and safety (#9) were prioritized. Designs 6 and 8 earned a "+" for supporting two or more degrees of freedom, while designs 2, 3, 4, and 7 received a "-" due to their simplicity or limited arm movement capabilities. For lightweight design (#2), only designs 2 and 3 scored a "+" because they used minimal material, whereas most other concepts were rated as "0." Regarding range of motion (#6), many designs were marked with a "-" due to challenges in working with shape memory alloys and restricted movement.

Safety (#9) was evaluated based on body motion and the complexity of the control mechanisms used. After going through all of the screening criteria, designs 2, 6, and 9 were ranked the highest and chosen to move forward in the iteration process.

Table II: Screening Criteria

	Concept Variants									
Selection Criteria	**1 (REF)**	**2**	**3**	**4**	**5**	**6**	**7**	**8**	**9**	**10**
#1 Number of degrees of freedom on an arm (2)	0	-	-	-	0	+	-	+	0	0
#2 Lightweight	0	+	+	-	-	0	0	0	0	-
#3 Uses soft materials	0	+	+	+	+	0	+	+	+	-
#4 Portability	0	0	0	0	0	0	0	0	0	-
#5 Ease of manufacture	0	-	-	+	-	-	-	-	-	-
#6 Range of motion	0	0	-	+	-	0	0	-	-	-
#7 Durability	0	0	0	-	-	0	-	-	0	+
#8 Ability to interpret human intention	0	-	-	-	+	+	+	+	0	0
#9 Safety	0	+	+	-	0	0	-	-	+	0
#10 Battery life	0	+	+	0	+	0	+	+	+	-
PLUSES	0	4	4	3	3	2	3	4	3	1
MINUSES	0	3	4	5	4	1	4	4	2	6
NET	0	1	0	-2	-1	1	-1	0	1	-5
RANK	6	2	4	9	7	3	8	5	1	10
CONTINUE?	No	Yes	No	No	No	Yes	No	No	Yes	No

Table III: Scoring Criteria

		New Ideas									
		2+		6+		9+		2-3 Hybrid		8+	
Selection Criteria	Weight	Rating	Weighted Score	Rating	Weighted Score	Rating	Weighted Score	Rating	Weighted Score	Rating	Weighted Score
#1 Number of degrees of freedom	0.1	4	0.4	3	0.3	4	0.4	3	0.3	3	0.3
#2 Lightweight	0.1	2	0.2	3	0.3	2	0.2	2	0.2	3	0.3
#3 Uses soft materials	0.1	4	0.4	4	0.4	4	0.4	4	0.4	4	0.4
#4 Portability	0.05	3	0.15	2	0.1	3	0.15	3	0.15	3	0.15
#5 Ease of manufacture	0.05	2	0.1	4	0.2	2	0.1	3	0.15	3	0.15
#6 Range of motion	0.15	5	0.75	3	0.45	3	0.45	4	0.6	2	0.3
#7 Durability	0.15	2	0.3	3	0.45	2	0.3	1	0.15	4	0.6
#8 Ability to interpret human intention	0.05	3	0.15	5	0.25	5	0.25	3	0.15	4	0.2
#9 Safety	0.15	5	0.75	3	0.45	5	0.75	5	0.75	5	0.75
#10 Battery life	0.1	4	0.4	3	0.3	4	0.4	3	0.3	3	0.3
Total Score		3.6		3.2		3.4		3.15			
Rank		1		4		3		5		2	
Continue?		Yes		No		No		No		No	

After rating the new iterations, we chose design 2+ as our final design. This decision was influenced by several factors. Once we determined that pneumatic actuation was the most

suitable technique for our project, it removed ideas 6+ and 8+ from consideration. Following this, we evaluated the remaining designs based on the predefined scoring criteria. Design 2+ was selected because it received the highest overall rating and thus aligned best with our project specifications. As detailed later in the report, the design evolved during the CAD modeling and assembly process, but this served as the initial inspiration.

Initial Specifications

Table IV: Initial Device Specifications with Associated Importance Levels

#		Specification Description	Importance* (1 = High, 3 = Low)
1	Ergonomics	The device is lightweight.	1
2		The device uses soft materials.	1
3		The device is comfortable.	1
4		The device is adjustable.	2
5		The device is capable of providing a force equal to twice or greater the average weight of a person's arm.	1
6		The device assists with rehabilitation.	1
7		The device is compliant with natural human frame and motion.	1

8	Functionality	The device has limitations on acceleration to protect the user.	1
9		The device assists with upper limb motion.	1
10		The device assists the wearer with at least one degree of freedom.	1
11		The device provides the same full range of motion (ROM) as a human joint.	2
12		The device has a minimum lifetime of 2000 cycles.	2
13		The power source lasts through multiple therapy sessions.	3
14		The device is capable of interpreting and predicting human intention and responding accordingly.	3
15		The device is able to lift small objects.	3
16		The device is portable.	3
17	Manufacturing	The device is affordable.	2
18		The device is environmentally friendly.	3
19		The device uses commonplace manufacturing techniques.	3

20		The device uses easily replaceable parts.	3

Final Specifications

Table V: Final Design Specifications and Performance Criteria

	Category	Metric	Units	Value
1	Ergonomics	The device is lightweight.	lbs	≤5
2		The device uses soft materials.	material type	pneumatic tubes, padding, and Velcro
3		The device is comfortable.	subject	≥3
4		The device is adjustable.	in	>3
5		The device is capable of providing a force equal to twice or greater the average weight of a person's arm.	lbs	>16
6		The device assists with rehabilitation.	subject or physical therapist	supports repetitive exercises
7		The device is compliant with natural	degrees	≤ 90

	Functionality	human frame and motion.		
8		The device has limitations on force to protect the user.	N	≤45
9		The device assists with upper limb motion.	upper body	shoulder
10		The device assists the wearer with at least two degrees of freedom.	DOF	≥2
11		The device includes a control system for initiating arm movement.	Control method	Joystick
12		The device allows variable control of arm movement speed.	Speed regulation method	Control code
13		The power source lasts through multiple therapy sessions.	hours	≥4
14		The device uses an actuation method fit for shoulder motion.	method of actuation	pneumatic muscles
15		The device uses parts that are resistant to fracture.	safety factor	≥3
16		The power source outputs sufficient	psi	≥20

		energy to cause contraction in the actuator.		
17	Manufacturing	The device is affordable.	US$	≤1200
18		The device uses materials that are readily available.	time to deliver	<2 weeks
19		The device uses commonplace manufacturing techniques.	manufacturing technique	3D printing, machining
20		The device uses easily replaceable parts.	part types	ABS plastic or parts bought from reliable online stores (McMaster Carr, Amazon)

Technical Analysis and Prototypes

Mechanical Structure

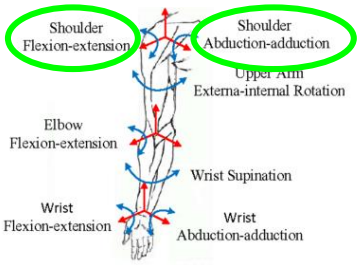

For our capstone project, the aim was to assist the user with at least two degrees of freedom in the shoulder: flexion/extension and abduction/adduction. The group decided to focus on designing a soft wearable exoskeleton for rehabilitation purposes aimed at patients with restricted motion in their arm who need consistent therapeutic sessions. This exoskeleton could allow patients to conduct more exercises per session, potentially accelerating the rehabilitation process.

After establishing the use-case scenario and defining the required degrees of freedom (DOF) for the shoulder rehabilitation, pneumatic artificial muscles were selected as the actuation method (see *Actuation Techniques* for further detail). The mechanical structure was then designed to interface effectively with these actuators while maintaining modularity and user comfort.

The design consists of five key components, all created using Computer-Aided Design (CAD):

1. Collar – consisting of a central back piece and two shoulder pieces,
2. Shoulder Hinge,
3. Shoulder Lever,
4. Back Muscle Connector, and
5. Muscle Clamp.

These components are labeled on the physical prototype in Fig. 3 and shown in CAD form in Fig. 4.

The collar serves as the structural base, wrapping around the upper back and shoulders and securing to the user with Velcro straps threader through slits at the front and back. The shoulder hinge connects to the collar via a snap-fit mechanism. It features a square peg-and-hole array that allows for adjustable positioning in multiple directions, enabling customization of the shoulder's DOF.

Once the hinge is snapped into the collar, the shoulder lever is mounted onto the hinge using a metal rod secured by two shaft collars (hardware elements functionally similar to nuts but lacking internal threading). The lever's contoured top supports the pneumatic muscles, which are routed and secured via muscle clamps using screws and locknuts at each end.

As the actuators inflate and deflate, the shoulder lever pivots about the hinge, replicating shoulder elevation and abduction (or flexion) motions. The design incorporates two pneumatic muscle pathways: one routes laterally to an elbow brace, while the other wraps over the shoulder toward the user's back and opposite shoulder. This dual-muscle configuration enables a broader range of arm elevation than a single actuator would allow. The elbow brace itself can be rotated and locked in place to further control limb positioning during use.

To support the control hardware, we also used CAD to create a dedicated electronics housing board (Fig. 10), designed to accommodate a full-length breadboard, air pump, solenoid valve, relay board, and an Arduino microcontroller. Although this board is not physically connected to the collar or shoulder assembly, it plays a critical role in organizing and securing the electronic components necessary for system operations.

Fig. 3 shows the fully assembled prototype with actuators integrated, while Fig. 4 displays the CAD model of the mechanical components alone. These visualizations illustrate both the functional layout and the modular design strategy of the system.

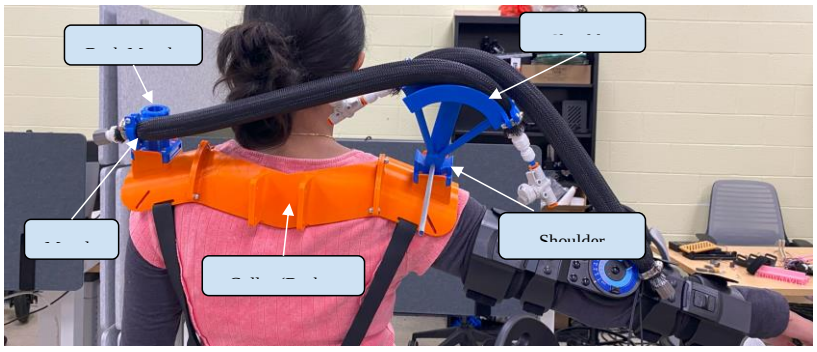

Fig. 3. Image of prototype after muscles were fully inflated with CAD pieces labeled.

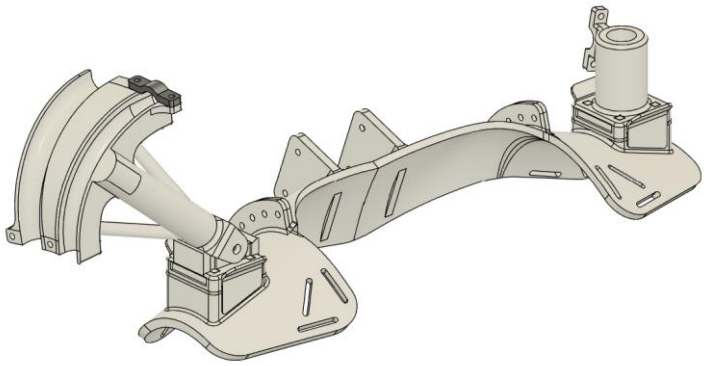

Fig. 4. CAD assembly of final design iteration. Pneumatic muscles are not shown.

Design Iterations

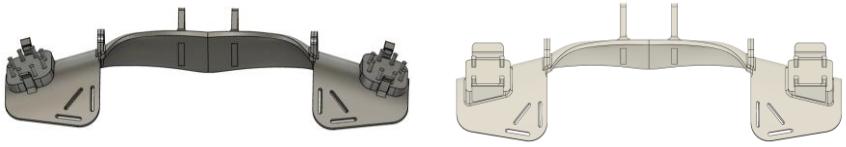

Fig. 5. Main collar for the exoskeleton. Initial design on the left, final design on the right.

Fig. 6. Muscle hinge and clamp designs. The image on the left and center were muscle clamps that were used in the initial design, when the muscle clamps could rotate at the end of the lever. The image on the right shows the final iteration of the muscle clamp, designed to attach to the end of the curved muscle path.

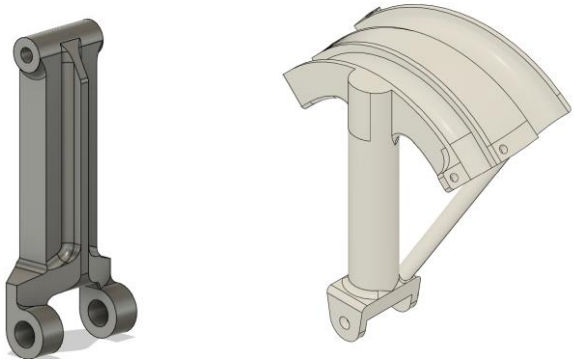

Fig. 7. Shoulder lever design. The initial design (left) had an extra joint at the top to allow the muscle clamps to rotate. The final design (right) opted for a fixed design that allowed the muscles to arc instead.

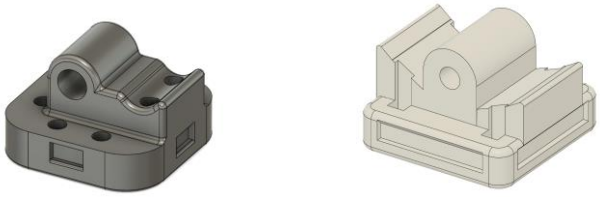

Fig. 8. Shoulder hinge connection pieces. The initial is shown on the left and the final is shown on the right.

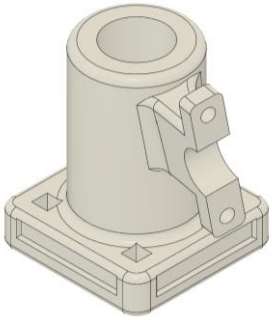

Fig 9. Back muscle connector which connects to the end of the back muscle to the left shoulder snap joint.

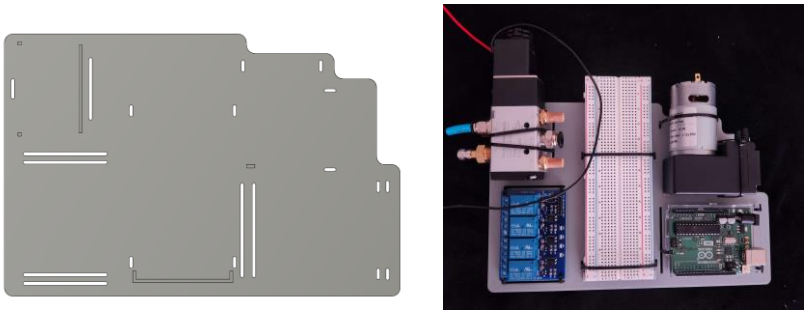

Fig. 10. Electronics housing board. This is designed to hold a full length breadboard, air pump, solenoid, Arduino, and a relay board.

Actuation Techniques

Two main actuation methods were considered to generate the force necessary for moving the arm. The first was shape memory alloy (SMA), which can be deformed but returned to its original shape by heating. SMA is lightweight, small, noiseless, and inexpensive, but movement is slow and difficult to control. Research indicates that SMA is better suited for wrist control, a degree of freedom not prioritized in this design (Bardi et al., 2022). Because SMA relies on heating to generate motion, it poses a potential safety risk, such as the user being burned, that would need to be carefully mitigated. Additionally, SMAs typically produce less force than pneumatic actuators and are therefore less suitable for applications requiring significant load-bearing capacity.

For these reasons, pneumatic actuators were chosen instead. A design called McKibben muscles will be applied. McKibben muscles are fabricated using a molded tube made from materials polymers or silicone on the inside and a layer of braided mesh on the outside. The mold provides shape and an airtight bladder, while the braided mesh provides tensile strength. An image of a McKibben muscle made by the 2022 Capstone team can be seen in Fig. 11. Pneumatic actuators operate by using compressed air to drive a system, and they appear to be

favored for movement in the shoulder. They can contract, expand, elongate, and bend when inflated (Bardi et al., 2022).

Control

The exoskeleton's control system can be implemented through multiple approaches. While some designs utilize closed-loop control with inertial measurement units (IMUs) and complex dynamic modeling for preprogrammed movements, we determined that an open-loop control scheme would be more appropriate for this application. Stroke rehabilitation often involves repetitive, patient-specific tasks - such as transferring water between bowls or performing arm raises - that vary significantly between individuals. An open-loop system, which allows real-time user control

Fig. 11. Change of length test of a McKibben muscle conducted by the 2022 Capstone team (Applegate et al., 2022).

rather than relying on preprogrammed motions, provides greater flexibility to accommodate these individualized therapeutic needs.

Additionally, this system is designed for at-home use, unlike traditional rigid exoskeletons that are typically confined to clinical settings. By avoiding complex programming requirements, the open-loop approach reduces barriers to accessibility and empowers users with greater freedom in their home-based therapy.

The exoskeleton employs a glove-mounted joystick positioned in the user's palm, enabling intuitive control of hand movements. The joystick generates an analog output ranging from 0 (fully depressed) to 1020 (fully extended), which is processed by an Arduino microcontroller to command arm actuation. Motion is achieved through a solenoid valve and DC micro pump: contraction occurs when the solenoid closes and the pump activates, while opening the valve releases pressure for extension. The descent speed is modulated by adjusting the valve's opening and toggling the pump during deflation - keeping the pump engaged slows the release.

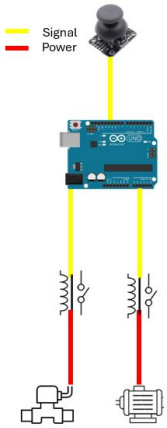

Fig. 12. Circuit Diagram of control system

To enhance system robustness, a programmable potentiometer could be integrated to dynamically adjust the pump's input voltage based on joystick displacement, allowing finer control over actuation speed and force.

Testing

Commented [1]: analysis on artificial muscle design: length, diameter. what force can we generate with what we have?
(what is the equation for calculating the force? refer to previous group's technical report?

FEA for CAD, generate enough force and torque to rotate whole arm: if i want to rotate, calc mass moment of inertia and angle to know force and moment (torque). is it the same force as generated by muscles? calculate moment needed for adduction/abduction

moment*theta : moment = F*d
(STATIC calculations^^)

refer to paper sarah gave for dynamics

Three primary methods of testing were used throughout the semester, one for each subcategory of the design: mechanical structure, actuation, and control. These tests were used to determine whether certain specifications were met and to ensure the safety of the device. Once each category was tested individually, a final test of the entire prototype was conducted on different users. Regarding mechanical structure, Finite Element Analysis (FEA) was used to determine regions where the stress concentrations were highest amongst the 3D printed parts. For actuation, after the pneumatic muscles were constructed and sealed, we used the air pump to inflate the tubes and measure the contraction length. The control system was tuned by adjusting solenoid settings for smoother movement.

Images of the final prototype, with the control system incorporated, are shown in Fig. 13. Following its completion, we conducted a series of trials on three different users to test the device's range of motion and the degrees of freedom it provides. Additional trials demonstrated the solenoid's ability to inflate and deflate the muscles without manual interference and explored whether the deflation speed could be effectively regulated through the use of simple code. The exoskeleton was tested on both male and female users of varying heights and weights to demonstrate its adjustability. The following sections provide detailed descriptions of the FEA, pneumatic actuation testing, and user trials conducted to evaluate the exoskeleton's mechanical performance and control system.

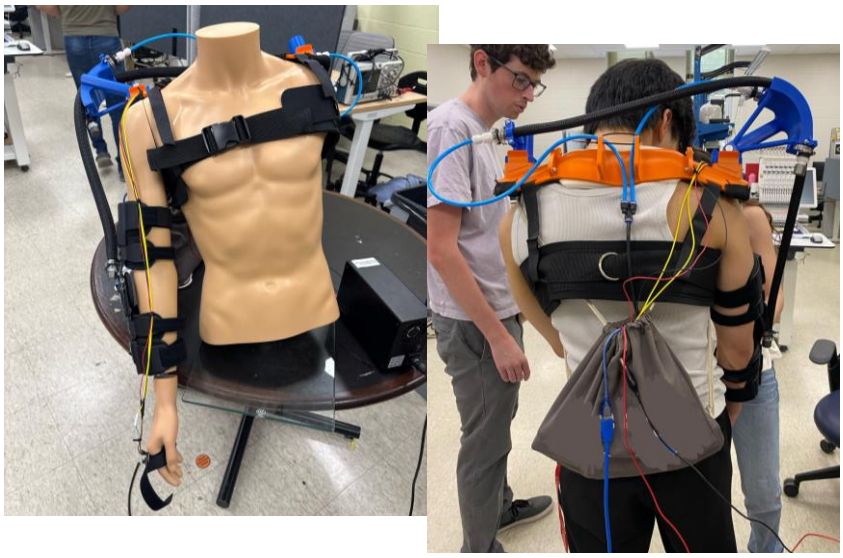

Fig. 13. Image of the front view of the final prototype, showing the wires and joystick used in the control system, shown on the left. The joystick is connected to a Velcro strap that wraps around the user's hand. Image of the back view of the prototype is shown on the right. The electronics for the control system are located within the bag.

a. Finite Element Analysis

A unique feature of our design is the ability to reposition the pneumatic muscles so that it can actuate in the direction of flexion and extension. The design achieves this by using snap-fit connections to the shoulder hinge. These snap fits need to be designed in a way such that they can withstand repetitive deformation from the user replacing the shoulder hinge. To test this, we performed a simple finite element analysis (FEA) on the snap fits. The initial design of this snap fit had a thickness of 0.6 mm. Fig. 14 shows the deformation plot of the snap fit.

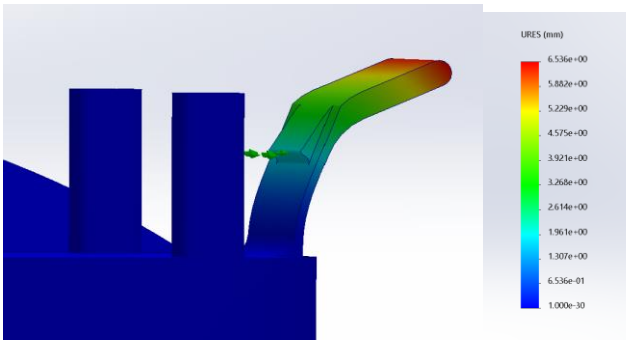

Fig. 14. Deformation plot from FEA analysis of the snap fit.

We used SOLIDWORKS to perform the FEA on the snap fit. The FEA was set up to simulate a prescribed displacement of 2 mm at the point where the snap fit would contact the shoulder hinge. The 2 mm is the maximum displacement that would be experienced by the hinge.

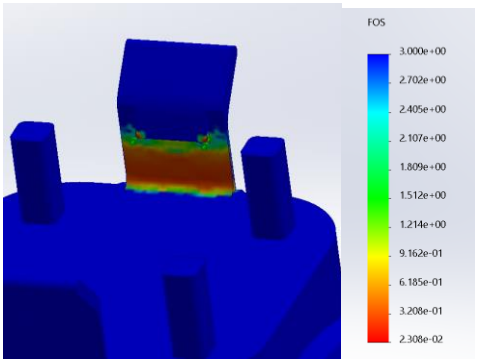

Fig. 15. Factor of safety plot from FEA analysis of the snap fit.

Fig. 15 shows the resulting factor of safety plot using Maximum Shear Stress (MSS) criteria for a conservative estimate. As we can see, the factor of safety gets dangerously low in the middle of the snap fit hinge. The FEA suggests that the part would yield at the middle section of the snap fit, where the factor of safety goes below one. However, upon printing and testing a prototype, we discovered that the part broke in a different area. Rather than breaking in the middle, the snap fit broke towards the bottom, where the fillet connected to the base of the shoulder hinge. This result does not align with the FEA's prediction. We believe it could be for the following reasons:

1) The FEA does not account for 3D printing geometry (infill patterns, layer lines, wall thicknesses). The material properties of a 3D printed object are very far from isotropic. Ideally, the most correct way to perform an FEA on a 3D printed object would be to put the object through a 3D printing slicer and get its gcode, then convert that gcode back into a 3D model which can be analyzed through FEA. However, there is currently no software that does this.

2) The material properties of the ABS material used for the FEA was estimated. The actual material properties of the ABS used for 3D printing may differ. Additionally, factors such as the temperature of the 3D printer may affect its strength as well, even if the material does not differ.

Due to these two substantial reasons, it is not entirely surprising that the FEA does not align with the real world result. As such, we used the results of the FEA as a very rough estimate when deciding how to approach the design of the snap fit. Additionally, physical testing showed that the snap fit deformed too easily because of its thinness and did not do a good job of holding in the shoulder hinge.

Based on the FEA results and the results of physical testing, we adjusted the design by making the body of the snap fit a little thicker (increasing from 0.6 mm to 0.8 mm) and also wider (increasing the width from 15 mm to 35 mm). The increased thickness allowed the snap fit to hold its position better once it was snapped in, and the increase in width would provide more area for the bending stress to be distributed.

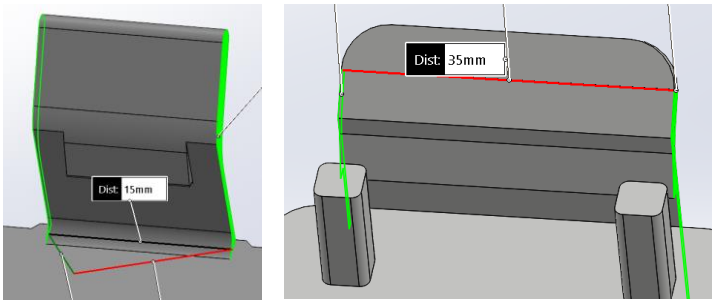

Fig. 16. Increase in the width of the snap fit (15 mm to 35 mm).

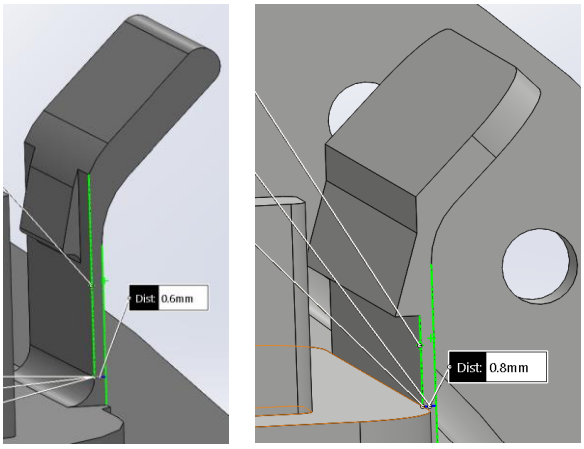

Fig. 17. Increase in snap fit thickness (0.6 to 0.8mm)

After printing and testing the prototype of the new snap fit, we found that they are a little tight, but performed adequately as far as repetitive deformation.

b. Pneumatic Muscle Contraction

Before integrating the pneumatic muscles into the mechanical structure of the exoskeleton, we tested them independently by connecting each to an air pump to measure their contraction lengths at full inflation. The power supply delivered 12V to the air pump, which operated at a maximum pressure of 220 kPa. Contraction lengths were measured using a tape measure. This testing was essential for two main reasons. Foremost, it allowed us to estimate the range of motion the exoskeleton could provide, given that pneumatic actuators provide linear motion. Second, it helped identify any air leaks and ensure that each muscle was properly sealed. The first muscle, extending from the top of the shoulder to slightly below the elbow, measured

21 inches in its resting state and 16.75 inches long when fully inflated. Both the resting and contracted states of the first muscle are shown below in Fig. 18.

Fig. 18. Muscle one contraction testing. 21” resting (top) and 16.75” at maximum contraction (bottom).

The second muscle, which spanned from shoulder to shoulder across the upper back, was 24.5 inches long and contracted to 20 inches. The resting and contracted states of this muscle are shown in Fig. 19.

Fig. 19. Muscle two contraction testing. 24.5” resting (top) and 20” after contraction (bottom).

Initial testing revealed small leaks that slowed the inflation process, but those were quickly resolved by tightening the metal zip ties securing each end of the muscle. A second issue arose during early prototype testing: the muscles were unable to fully contract due to insufficient curvature in the CAD-designed mounting brackets. This misalignment restricted muscle actuation, thereby reducing the achievable range of motion. Since pneumatic muscles follow a linear path, they require smooth, curved mounting surfaces to operate the most effectively. After redesigning the hinge component to incorporate longer curves for the muscles to rest on, the alignment issue was resolved. The muscles then performed as expected, generating our desired range of motion.

The 220 kPa supplies sufficient pressure to generate a force great enough to lift the arm assuming the arm remains limp and there is no air leakage. At maximum contraction the diameter of the muscle is 1 inch, generating 100.2 pounds of force according to the equation $pressure = force/area$. The 100.2 pound force acts approximately 20 inches down the arm. The average human arm is 39.4 inches in length, 8 pounds in weight, and has a center of mass 14.6 inches away from the center of rotation in the shoulder (ExRx). The force generated by the pump causes clockwise torque (for the right arm), while the weight of the right arm generates counterclockwise torque. As the arm is lifted, some of the 100.2 pounds of force acts in the x-direction, but even when maximum contraction is reached the net upward force is great enough to oppose the downward gravitational forces allowing the arm to remain stable. Once maximum contraction on the artificial muscle is reached, the system will remain in equilibrium with no forces causing dynamic motion anymore. This can be seen in Appendix VI.

c. User Testing and Video Analysis

To ensure repetitive motion and that final specifications were met, we tested the final prototype throughout numerous trials. We used Pasco software to perform a video analysis on each of these trials. For shoulder abduction, a female user wore the exoskeleton while we performed five trials on the ROM generated by the first muscle, five trials on the additional ROM generated by the second muscle, and five trials on the ROM generated by the two muscles inflated in tandem. There were two primary purposes of testing the muscles separately and then in conjunction: first, to ensure the muscles were individually performing as expected; and second, to use the achieved angles of the first two muscles to predict the final angle of the lifted arm. Angle versus time graphs were used to determine the angle of the arm in degrees from its initial resting position to its final position over time. The graphs were expected to show a linear trend. Each muscle was expected to individually reach approximately 40-45 degrees from their resting positions; when activated together, a range of 80-90 degrees was anticipated. Images of these graphs can be found below in Fig. 20.

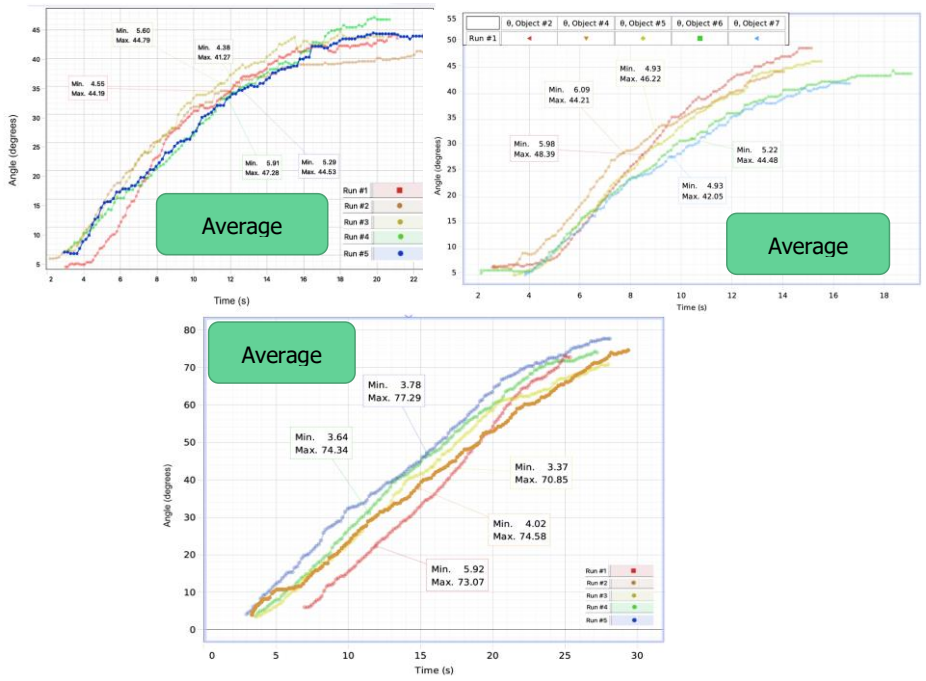

Fig. 20. Angle versus time graphs for shoulder abduction for muscle one (top left), muscle two (top right), and the muscles combined (bottom). Maximum and minimum values for data points labeled. Average maximum angles for each trial listed on each graph.

The results matched our predictions. The data followed a linear trend, with small exceptions shown among the beginning and end data points. This is because we started tracking before the air pump was turned on for some of the trials, and we continued marking data points even after the muscles had fully inflated to ensure we captured the maximum angle. The first muscle had an average maximum angle of 39.27 degrees, the second muscle had an average maximum angle of 39.64 degrees, and both muscles had an average maximum angle of 69.88 degrees. The average maximum angles were calculated by subtracting the minimum angle value

from the maximum angle value for each trial and finding the average of those five numbers. The reason for subtracting the minimum angle was to account for the natural resting state of the arm in the brace, which was around five degrees. We wanted to show as close to the exact angle that the muscles could generate by themselves. Without subtracting the minimum angle values, the average maximum angle would be about five degrees higher. If the resting state of the arm is included, the resultant angle values align with the upper end of our predicted range. Even without the resting state, the values remain close to expectation. The only discrepancy is the maximum angle achieved by both muscles, which was smaller than expected. This is likely related to the shifting of the collar over the course of many trials. The exoskeleton has a slight imbalance in weight distribution, leaning more toward the side with the shoulder lever, which causes it to gradually shift. Upon later review of the video, we observed significant collar movement during the trials involving both muscles, which clearly affected the arm's range of motion. Had the collar been securely repositioned before each trial, the arm likely would have reached a higher angle.

After determining the maximum achievable angle of the shoulder in abduction, Pasco software was again used to test the control system. Once it was known that the arm could reach the desired position, it was necessary to implement a control system that would inflate and deflate the muscles on command to reach the goal of repetitive movement for rehabilitation. Additionally, when the muscles were deflated by manually disconnecting the air pump, the arm fell back to its resting state rather quickly. Because it was team members without shoulder injury using the exoskeleton, this did not matter. However, if the person using it had a real injury, this could be a safety hazard. For this reason, we chose to test the aspect of the control that regulated the speed at which the arm returned to its resting state. We had two modes: "fast" and "slow."

We made angle versus time graphs for three trials for each mode, and we measured the slope of each trial. The slope values represented the angular velocity of the arm. The slow mode was expected to have a smaller slope than the fast mode. Images of the graphs can be seen in Fig. 21.

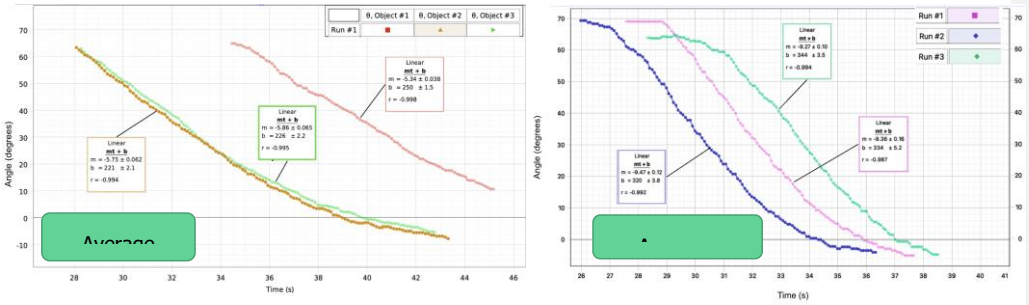

Fig. 21. Angle versus time graphs for shoulder adduction for the slow mode (left) and the fast mode) right. Slopes listed for each trial, and average slope values listed at the top left of each graph.

The results aligned with our predictions. The slow mode of the control system created a smaller angular velocity than the fast mode. These results showed that our control system could effectively regulate the speed of the muscle deflation, therefore ensuring the user's arm returns to its resting state at a reasonable pace. Additionally, this testing demonstrated that the control system can repeatedly inflate and deflate the artificial muscles to raise the arm to its maximum position and return it to its resting position, as well as hold the muscles in place at various arbitrary positions.

Once the testing was complete for shoulder abduction, we performed a trial to verify that the exoskeleton could perform flexion and extension when the shoulder lever was rotated forward using the snap fit portion of the collar. Only the muscle extending from the top of the

shoulder to just below the elbow was used for this test because the other muscle contorted to an unnatural angle when rotated, and we did not want to risk the user's safety. With just one muscle, we expected the arm to reach about 40-45 degrees. An image of the results of the trial can be seen in Fig. 22.

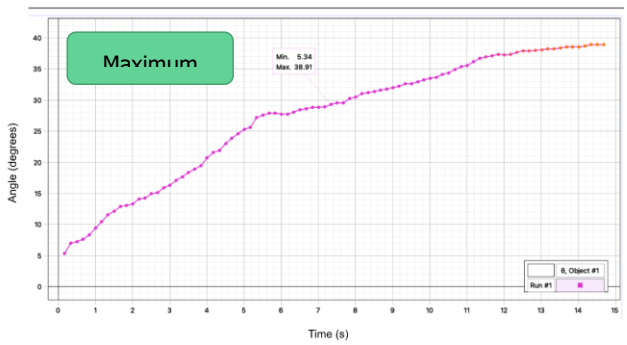

Fig. 22. Angle versus time graph for flexion and extension using only one muscle. Maximum and minimum data point values listed.

The results were slightly lower than expected but remained close to the expected range. Including the resting arm state, the arm reached an angle of approximately 39 degrees; excluding that state, the arm reached about 34 degrees. We believe this lower-than-expected angle may have been due to misalignment between the muscle and the shoulder lever, caused by the elbow brace. The muscle connected to the side of the brace and thus relied on the position of the brace during inflation. Because the brace was originally set up for abduction and adduction, it is likely that it was not repositioned adequately when switching the lever to enable flexion and extension. Consequently, the muscle did not form a straight line on the front side of the arm. Rather, it

formed a slight diagonal, which in turn prevented the arm from reaching its maximum position. Despite this, the arm still obtained a satisfactory range of motion in flexion and extension, solidifying the exoskeleton's ability to support two different degrees of freedom.

Specifications Met

Table VI: Verification of Top 10 Design Specifications

	Category	Metric	Units	Verification
1	Ergonomics	The device uses soft materials.	material type	Verified through use of pneumatic artificial muscles, padding underneath the shoulder collar, and Velcro straps for the harness.
2		The device is comfortable.	subject	Verified through a group survey (n=5); average comfort rating was 3.7 out of 5.
3		The device is adjustable.	in	Verified through the use of Velcro straps that the device allowed more than 3 inches of adjustability.
4	Functionality	The device assists with rehabilitation.	subject or physical	Verified through over 20 trials with 3 users; all participants

			therapist	completed target motions successfully with increased range of motion.
5		The device assists the wearer with at least two degrees of freedom.	DOF	Verified through user testing. The exoskeleton successfully enabled two DOF in the shoulder, achieving a maximum of approximately 77° in abduction/adduction and 39° in flexion/extension, including resting arm positions.
6		The device includes a control system for initiating arm movement.	Control method	Verified through the use of a joystick to control inflation and deflation of the muscles on command. Deflation operated in two modes: slow mode averaged 13.5 seconds and fast mode averaged 8.83 seconds to fully deflate across three trials.
7		The device uses an actuation method fit for	method of actuation	Verified through use of pneumatic muscles.

		shoulder motion.		
8	Manufacturing	The device is affordable.	US$	Verified through cost analysis. Individual device components are all under $70. All used components add up to under $250, which is much less than multiple in-clinic physical therapy sessions.
9		The device uses commonplace manufacturing techniques.	manufacturing technique	Verified by 3D printing and manually machining aluminum rods.
10		The device uses easily replaceable parts.	part types	Verified through modular CAD design, use of ABS plastic, and purchasing from reliable online stores (McMaster Carr, Amazon).

Summary and Conclusion

Accomplishments

At the beginning of the semester, our goal was to build a rehabilitative device that assists patients in achieving upper limb motion in two out of seven degrees of freedom in the arm, both in the shoulder (flexion/extension and abduction/adduction). By the end of the semester, our device was able to accomplish these two degrees of freedom through utilizing a snap fit shoulder piece. This shoulder piece could be taken out of its mount on the collar, rotated 90 degrees, and snapped back into place to switch between degrees of freedom because it changed the direction of the muscle and lifted the arms in two distinct ways. In terms of range of motion, our device is able to lift the arm up almost the full 90 degrees in abduction/adduction and about 45 degrees in flexion/extension. Incorporating two pneumatically actuated muscles - one going shoulder to elbow simulating the tricep and one going shoulder to shoulder simulating the lateral muscles - worked well for abduction/adduction because they pulled the arm up almost the full 90 degrees. In addition, having longer muscles allowed for more inflation, thus increasing how much the muscles could lift the arm up in both flexion/extension and abduction/adduction. Our collar design also worked as intended. As a whole, the collar fits on large and small body types. The padding we added works well and provides comfort for the user, especially as they go through the repetitive motions. The shoulder snap fit piece, as discussed in the previous paragraph, allowed for two degrees of motion. The curved, lever hinge gave the artificial muscles direction and helped it move along with the arm so it wouldn't get caught and limit range of motion.

Initially, each artificial muscle had to be inflated with the air pump separately. The shoulder to elbow muscle would be inflated first, lifting the arm up 45 degrees. Then the tube from the air pump would switch to the shoulder to shoulder muscle to lift the arm up about another 30 degrees for abduction/adduction. However, our control mechanism gave some

autonomy and control to the user. Using an Arduino microcontroller, we were able to create a circuit that allowed the user to stop and start the air pump, as well as control the speed at which the muscle deflated and let down their arm. The user controlled these motions with a joystick attached to the bottom of their elbow brace near their hand. This entire circuit, including the air pump, was housed in a small drawstring bag the user wore on their back.

Limitations

While we were able to achieve motion in both flexion/extension and abduction/adduction degrees of freedom, we were unable to achieve full 90 degree range of motion in flexion/extension because the shoulder to shoulder muscle did not provide a linear path to allow the arm to lift up in this degree of freedom. Additionally, repetitive motions for prolonged periods of time, as well an imbalance in weight on the collar, resulted in the collar constantly shifting slightly out of place and someone would have to help the patient adjust it. Besides mechanical limitations, the way we held our electronics and control components also did not work well. Our bread board, solenoid, relay, air pump, and corresponding connections were all placed into a bag that made it easy for wires to come loose. Component limitations prevented us from controlling how fast the muscles inflated because we were working with a constant pressure from our pump. In addition our power supply was large and bulky and could not fit in the electronics bag. This added another item the patient would have to carry, which is not ideal for our portable design.

Improvements and Future Work

To increase range of motion in flexion/extension, new actuation methods could be incorporated. Alternatively, the position of the back shoulder to shoulder muscle could be changed to go down the user's back, providing a linear path for the arm to lift up during this type

of motion. To prevent the device from moving as the patient does repetitive motions, stronger harnesses can be used to keep it in place, as well as a counterweight on the other shoulder to balance the collar. To consolidate electronics, a specific CAD structure/housing unit of each component can be made that groups similar components together. Other additions to the device could include mounting a motor and rotating turn plate to the collar to enable shoulder rotation (the third degree of freedom in the shoulder). Another artificial muscle could be added for elbow and wrist movement. To control variable output pressure from the air pump, engineers could add resistors as the user gains mobility (10% resistance, then 20%, etc.) All these changes can help make the device better and more versatile.

Appendix I: Bibliography

Antonelli, M. G., Beomonte Zobel, P., De Marcellis, A., & Palange, E. (2022). Design and Characterization of a Mckibben Pneumatic Muscle Prototype with an Embedded Capacitive Length Transducer. *Machines*, *10*(12), 1156. https://doi.org/10.3390/machines10121156

Applegate, C., Carley, J., Rojo, N., Lee, M., Nazari, I. (2022). Upper Limb Exoskeleton for Shoulder Joint Control. *The University of Virginia*. https://doi.org/10.18130/5xw7-m198

Bardi, E., Gandolla, M., Braghin, F., & et al. (2022). Upper limb soft robotic wearable devices: a systematic review. *Journal of NeuroEngineering and Rehabilitation*, *19*(87). https://doi.org/10.1186/s12984-022-01065-9

Body segment data. ExRx.net: Exercise Prescription on Internet. (n.d.). https://exrx.net/Kinesiology/Segments

Cappello, L., Binh, D. K., Yen, S.-C., & Masia, L. (2016). Design and preliminary characterization of a soft wearable exoskeleton for upper limb. In *2016 6th IEEE International Conference on Biomedical Robotics and Biomechatronics (BioRob)* (pp. 623–630). IEEE. https://doi.org/10.1109/BIOROB.2016.7523695

Chiaradia, D., Xiloyannis, M., Solazzi, M., Masia, L., & Frisoli, A. (2020). Rigid versus soft exoskeletons: Interaction strategies for upper limb assistive technology. In J. Rosen & P. W. Ferguson (Eds.), *Wearable robotics* (pp. 67-90). Academic Press. https://doi.org/10.1016/B978-0-12-814659-0.00004-7

Li, N., Yu, P., Yang, T., Zhao, L., Liu, Z., Xi, N., & (2017). Bio-inspired wearable soft upper-limb exoskeleton robot for stroke survivors. In *2017 IEEE International Conference on Robotics and Biomimetics (ROBIO)* (pp. 2693–2698). IEEE.

https://doi.org/10.1109/ROBIO.2017.8324826

Zhang, J., Xiao, X., Jin, Q., Li, J., Zhong, D., Li, Y., Qin, Y., Zhang, H., Liu, X., Xue, C., Zheng, Z., & Jin, R. (2023, April 18). The effect and safety of constraint-induced movement therapy for post-stroke motor dysfunction: A meta-analysis and trial sequential analysis. *Frontiers in neurology*. https://pmc.ncbi.nlm.nih.gov/articles/PMC10151521/

Appendix II: Assembly and BOM

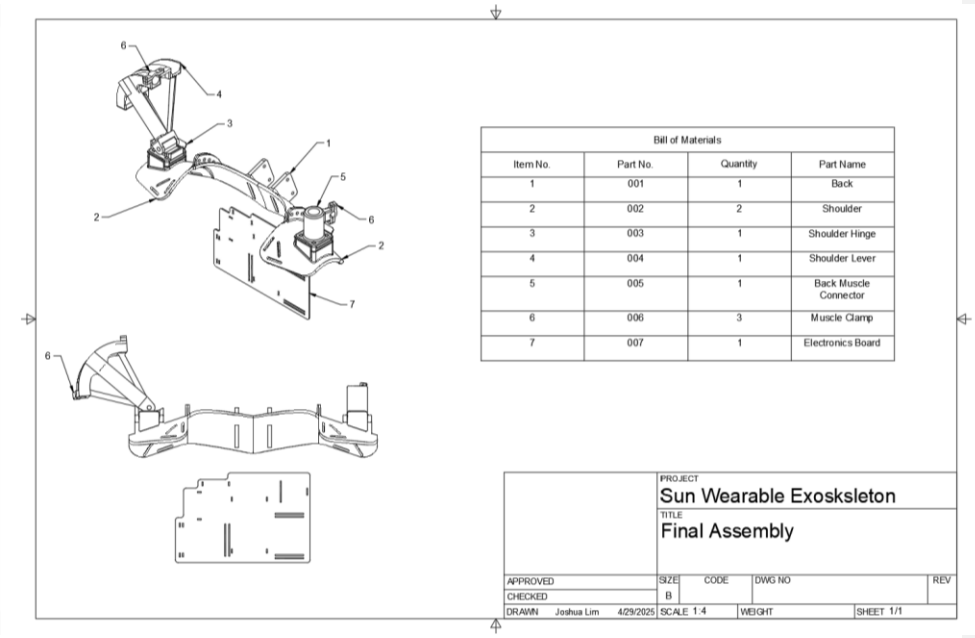

Bill of Materials			
Item No.	Part No.	Quantity	Part Name
1	001	1	Back
2	002	2	Shoulder
3	003	1	Shoulder Hinge
4	004	1	Shoulder Lever
5	005	1	Back Muscle Connector
6	006	3	Muscle Clamp
7	007	1	Electronics Board

PROJECT: Sun Wearable Exosksleton
TITLE: Final Assembly
APPROVED
CHECKED
DRAWN Joshua Lim 4/29/2025
SIZE B | CODE | DWG NO | REV
SCALE 1:4 | WEIGHT | SHEET 1/1

Fig.II.1. Final Assembly of 3-D printed parts

Part Number	Part Name	Quantity	Cost
001	Back	1	N/A
002	Shoulder	2	N/A
003	Shoulder Hinge	1	N/A
004	Shoulder Lever	1	N/A
005	Back Muscle Connector	1	N/A
006	Muscle Clamp	3	N/A
007	Electronics Board	1	N/A
008	Solenoid	1	N/A
090	Wires	10	N/A
010	Power Supply	1	N/A
011	Alligator Clips	2	N/A
012	Tubing to Air Pump	5ft	N/A
013	Airflow valve	1	N/A
014	Y-Connector	1	N/A
015	T-Connector	1	N/A
016	Drawstring Backpack	1	N/A
017	End Cap	2	N/A
018	Metal Zip Tie	4	N/A
743274437324	Pump	1	$26.52
8974K22	1/4" Aluminum Rod 1 ft	1	$1.96
90453A112	M4 Screws 12mm [Pack of 50]	1	$7.14
92832A574	M4 Screws 50 mm [Pack of 50]	1	$7.72
90453A112	M4 Nylock Nuts [Pack of 50]	1	$7.14
6432K12	1/4" Shaft Collars [Pack of 10]	1	$1.94
B0D3D4DH5J	4 Relay Board	1	$5.99
1528-5743-ND	Joystick	1	$7.50
B008GRTSV6	Arduino	1	$27.60
B01EV6LJ7G	Breadboard	1	$6.99
M000006	USB 2.0 Cable Type A/B	1	$7.60
B082V84H2V	Arm Brace	1	$69.96
B081JX568Y	Belt	1	$14.99
B0B93R3CYW	Velcro	1 (16ft)	$9.99
B0C3ZV7ZMY	Shoulder Padding	1 (Pack of 4)	$7.49
B0DGX6K1JX	Back Padding	1	$7.99
5234K26	Bladder	10 ft	$2.10
9284K615	Mesh	10ft	$7.15
5372K123	Plastic Tube Fitting	1 (Pack of 10)	$6.85
B015HLYJKS	Tube connector	1 (Pack of 5)	$7.99
		Total Cost	$242.61

Fig. II.2. Final Bill of Materials, including only the materials used in the final design.

Appendix III: Detailed Drawings

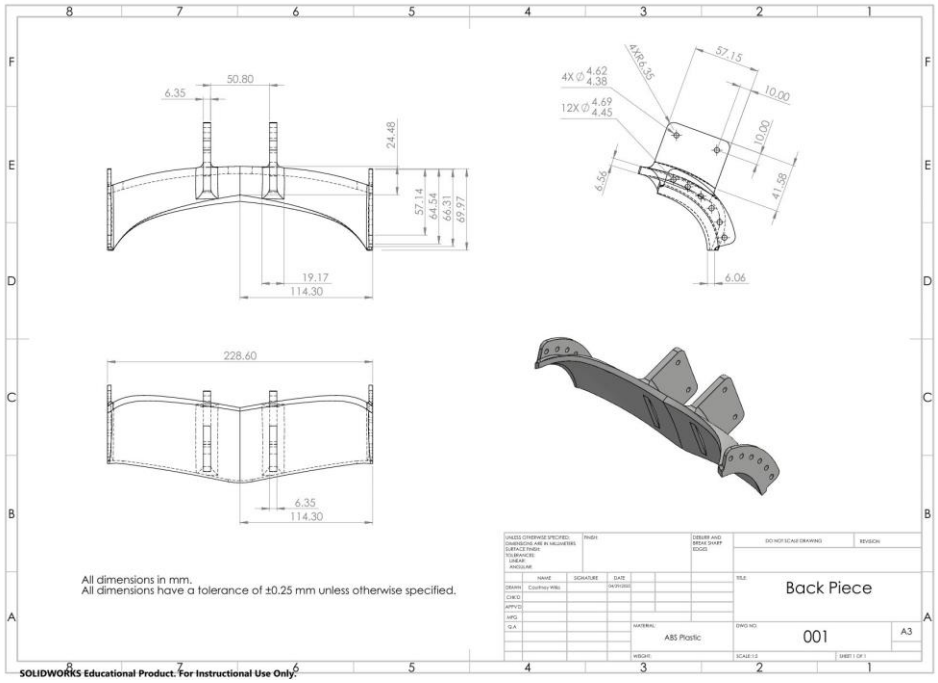

Fig.III.1. Detailed drawing of back collar piece

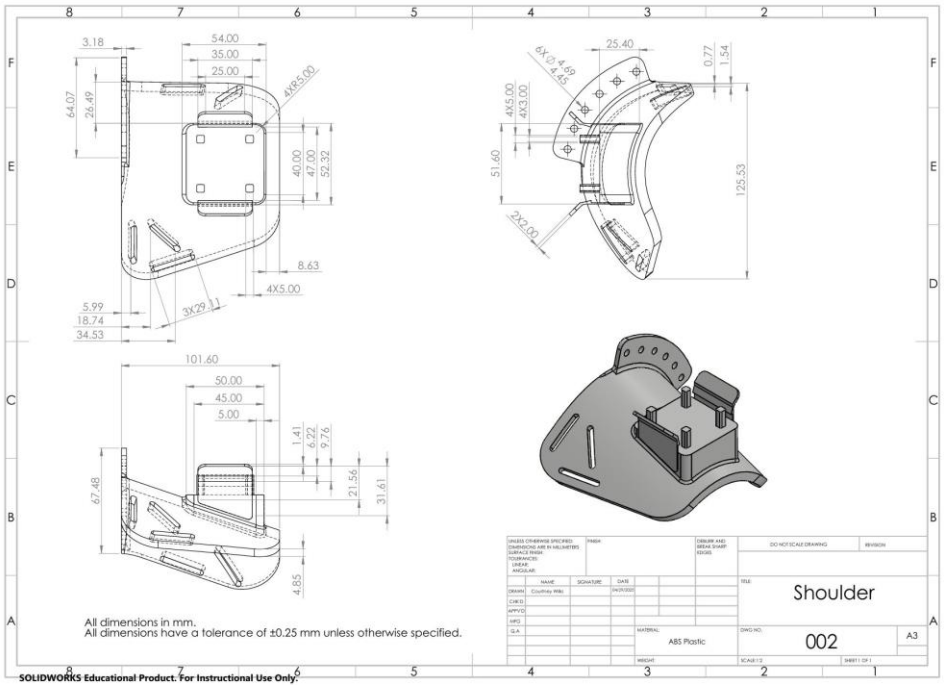

Fig.III.2. Detailed drawing of shoulder collar piece

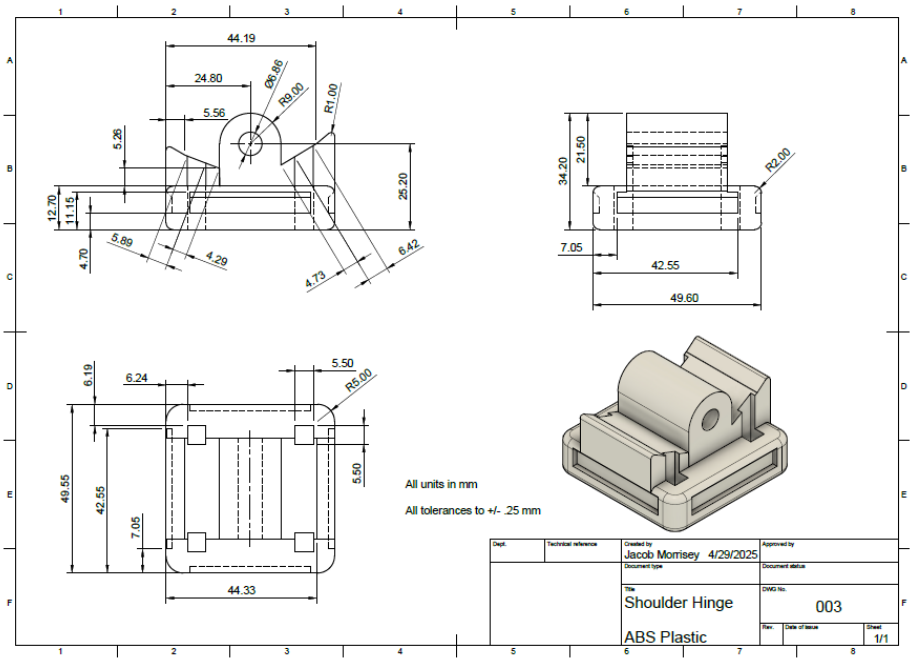

Fig.III.3. Detailed drawing of rotating shoulder hinge

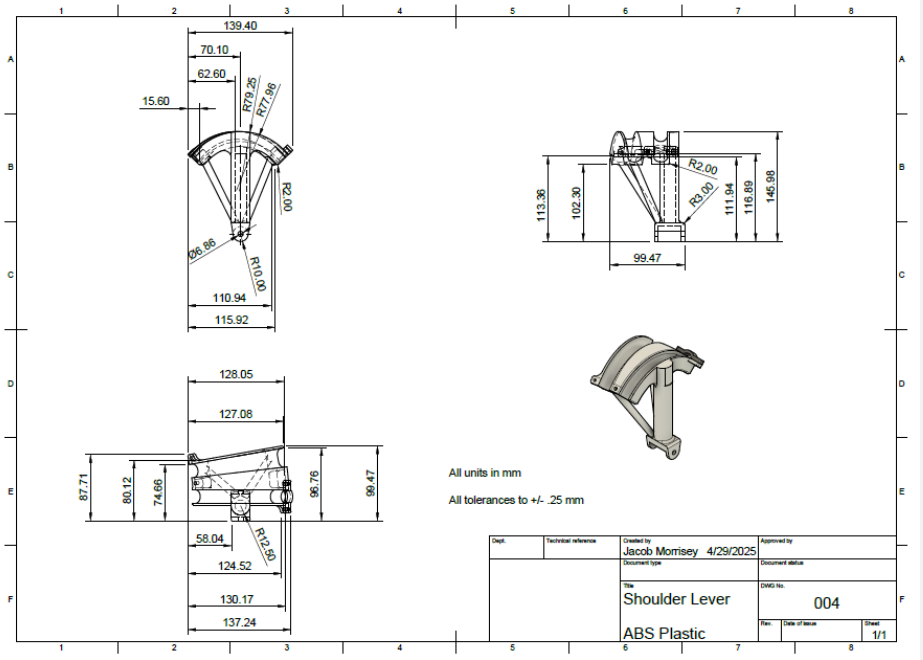

Fig.III.4. Detailed drawing of shoulder lever

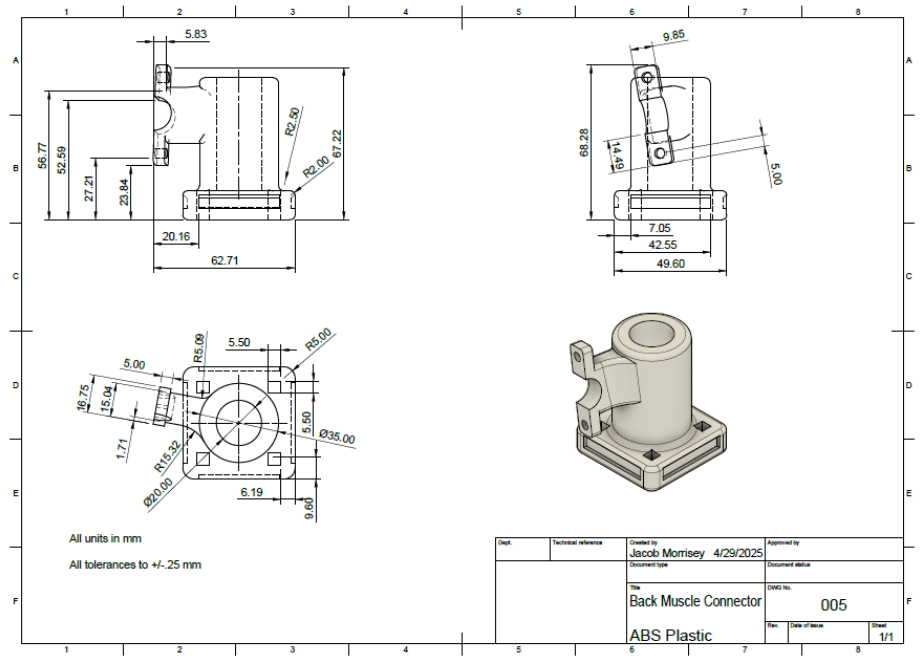

Fig.III.5. Detailed drawing of back muscle connector

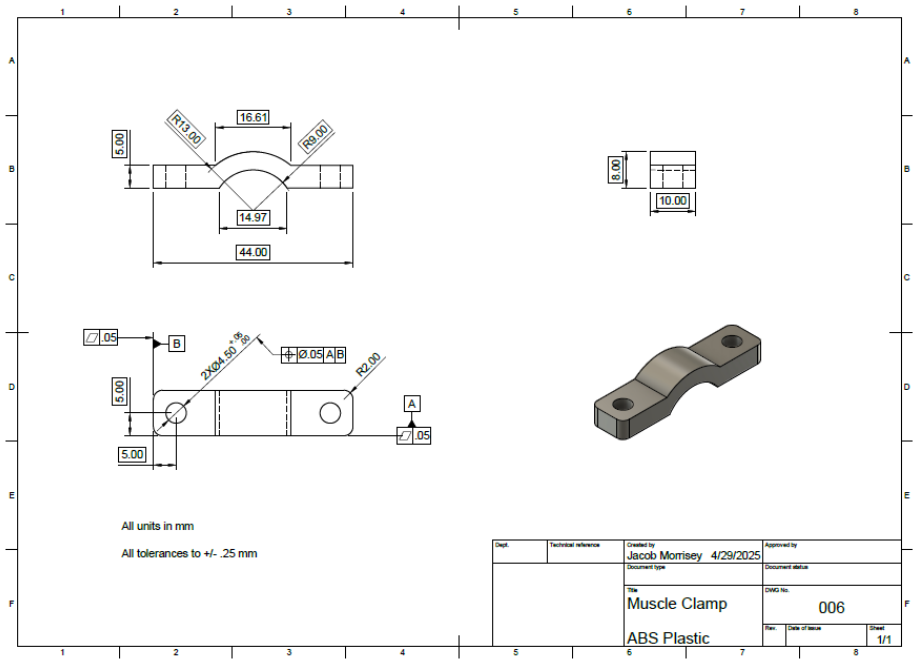

Fig.III.6. Detailed drawing of the muscle clamp

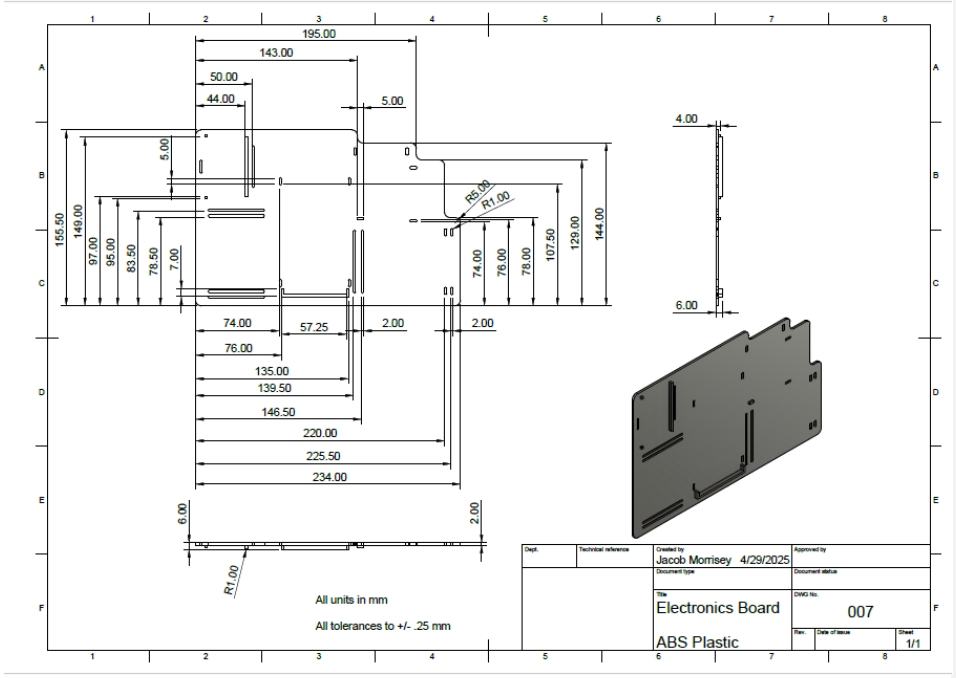

Fig.III.7. Detailed drawing of electronic components housing board

Appendix IV: Lagrangian Dynamics

$\mathcal{L} = KE - PE$, $KE = \frac{1}{2} m v^T v + \frac{1}{2} I \omega^T \omega$, $PE = mgh$

$\mathcal{L} = \frac{1}{2} m v^T v + \frac{1}{2} I \omega^T \omega - mgh$

$\Downarrow$

$\tau = \frac{d}{dt}\frac{\partial \mathcal{L}}{\partial \dot{\theta}} - \frac{\partial \mathcal{L}}{\partial \theta} = \boxed{D(q)\ddot{q}}$ (velocity term) $+ \boxed{C(q,\dot{q})\dot{q}}$ (friction term) $+ \boxed{G(q)}$ (gravity term)

- frame
- muscle
- joint
- measurements

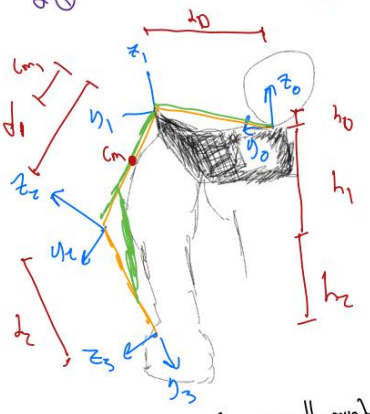

Shoulder 1

$R^0_1 = \begin{bmatrix} c_1 & -s_1 & 0 \\ s_1 & c_1 & 0 \\ 0 & 0 & 1 \end{bmatrix}$, $J_v = \begin{bmatrix} d_1 c_1 & 0 \\ d_1 s_1 & 0 \\ 0 & 0 \end{bmatrix}$ (J_{v1}), $J_\omega = \begin{bmatrix} 0 & 0 \\ 0 & 0 \\ 1 & 0 \end{bmatrix}$ (J_{v2} = zero all around)

$KE = \frac{1}{2}\dot{q}\left(m_1 J_{v_1}^T J_{v1} + J_\omega^T R_1^0 \left(I R_1^{0T} J_{\omega 1}\right)\right)\dot{q} = \frac{1}{2}\dot{q}^T D(q)\dot{q}$

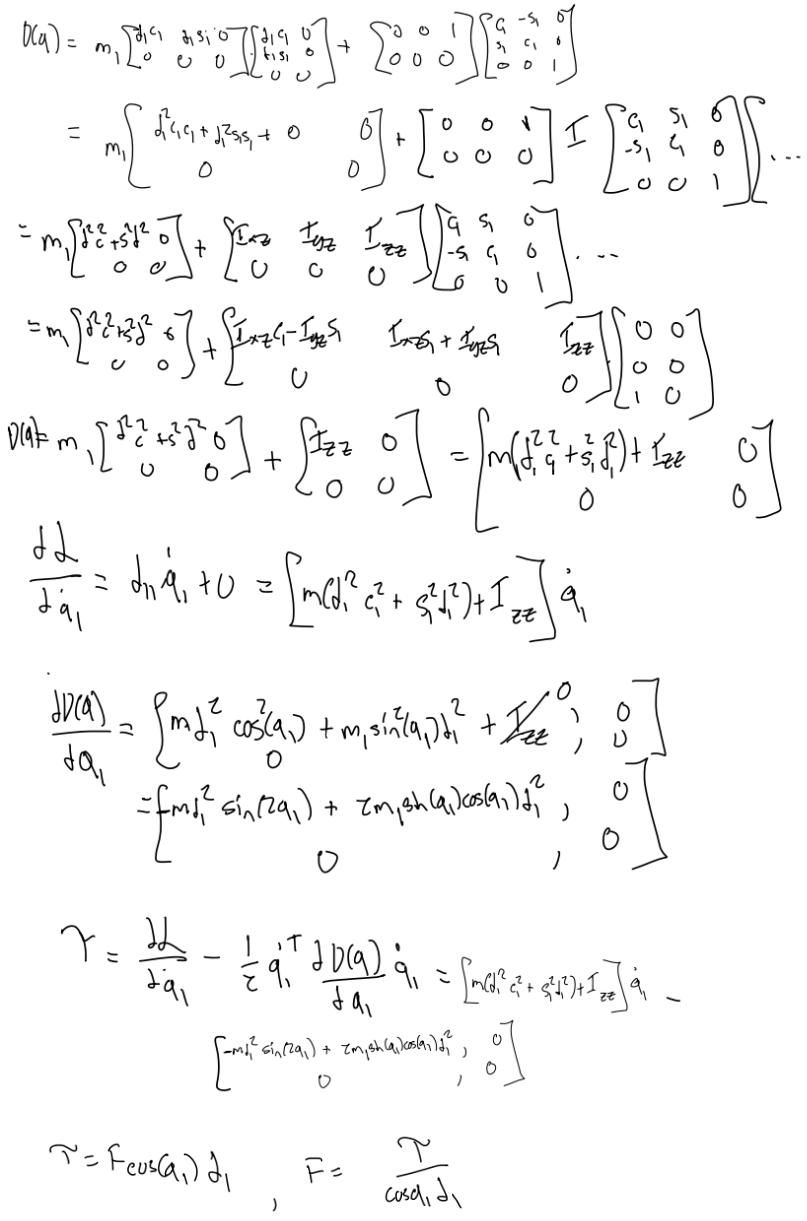

Fig.IV.1. Derivation of lagrangian dynamics used to define shoulder movement

Appendix V: Arduino Code

```
#include "Adafruit_seesaw.h"
Adafruit_seesaw ss;
#define BUTTON_X         6
#define BUTTON_Y         2
#define BUTTON_A         5
#define BUTTON_B         1
#define BUTTON_SELECT    0
#define BUTTON_START    16
uint32_t button_mask = (1UL << BUTTON_X) | (1UL << BUTTON_Y) | (1UL << BUTTON_START)
                       | (1UL << BUTTON_A) | (1UL << BUTTON_B) | (1UL << BUTTON_SELECT)
#define VALVE_PIN 5
#define PUMP_PIN  6
enum State {
  Inflate,
  Hold,
  SlowDeflate
};
State state = Hold;
unsigned long slowDeflateStart = 0;
void setup() {
  Serial.begin(9600);
  while(!Serial) delay(10);
  Serial.println("Gamepad QT example!");
  if(!ss.begin(0x50)) {
    Serial.println("ERROR! seesaw not found");
    while(1) delay(1);
  }
  Serial.println("seesaw started");
  uint32_t version = ((ss.getVersion() >> 16) & 0xFFFF);
  if (version != 5743) {
    Serial.print("Wrong firmware loaded? ");
    Serial.println(version);
    while(1) delay(10);
  }
```

```
  Serial.println("Found Product 5743");
  ss.pinModeBulk(button_mask, INPUT_PULLUP);
  ss.setGPIOInterrupts(button_mask, 1);
  pinMode(VALVE_PIN, OUTPUT);
  pinMode(PUMP_PIN, OUTPUT);
  digitalWrite(VALVE_PIN, LOW);
  digitalWrite(PUMP_PIN, LOW);

int last_x = 0, last_y = 0;
void loop() {
  delay(100); // throttle serial output
  int x = 1023 - ss.analogRead(14);
  int y = 1023 - ss.analogRead(15);
  if (abs(x - last_x) > 3 || abs(y - last_y) > 3) {
    Serial.print("x: "); Serial.print(x);
    Serial.print(", y: "); Serial.println(y);
    last_x = x;
    last_y = y;
  }
  if (y > 800) {
    // Joystick up -> Inflate
    state = Inflate;
    slowDeflateStart = 0;
  }
  else if (y < 200) {
    // Joystick down -> SlowDeflate
    if (state != SlowDeflate) {
      slowDeflateStart = millis();
    }
    state = SlowDeflate;
  }
  else {
    // Neutral position -> Hold
    state = Hold;
    slowDeflateStart = 0;
  }
```

```
switch(state) {
  case Inflate:
    Serial.println("State: Inflate");
    digitalWrite(VALVE_PIN, LOW);  // valve closed
    digitalWrite(PUMP_PIN, HIGH); // pump on
    break;

  case Hold:
    Serial.println("State: Hold");
    digitalWrite(VALVE_PIN, HIGH); // valve closed
    digitalWrite(PUMP_PIN, HIGH);  // pump off
    break;

  case SlowDeflate:
    Serial.println("State: SlowDeflate");
    digitalWrite(VALVE_PIN, LOW); // valve open
    digitalWrite(PUMP_PIN, LOW);  // pump on
    break;
}
uint32_t buttons = ss.digitalReadBulk(button_mask);
if (! (buttons & (1UL << BUTTON_A))) Serial.println("Button A pressed");
if (! (buttons & (1UL << BUTTON_B))) Serial.println("Button B pressed");
if (! (buttons & (1UL << BUTTON_Y))) Serial.println("Button Y pressed");
if (! (buttons & (1UL << BUTTON_X))) Serial.println("Button X pressed");
if (! (buttons & (1UL << BUTTON_SELECT))) Serial.println("Button SELECT pressed");
if (! (buttons & (1UL << BUTTON_START))) Serial.println("Button START pressed");
```

Fig.V.1. Arduino code used for control system

Appendix VI: Free Body Diagrams

220 KPa = 31.9 psi $P = \frac{F}{A}$

$31.9 = \frac{F}{\pi \cdot 1^2}$ F = 100.2 lb

At rest:

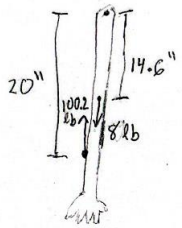

100.2lb · 20" − 8 lb · 14.6"

τ = 1887.2 lb·in

At 45°:

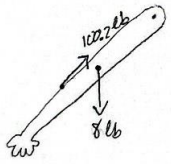

100.2 sin(45) · 20" − 8 · 14.6"

τ = 1300 lb·in

Fig.VI.1 Free Body Diagrams with Torque Calculations